NASA TECHNICAL NOTE

NASA TN D-3626

NASA TN D-3626

ANALYSIS OF NONCONSTANT AREA COMBUSTION AND MIXING IN RAMJET AND ROCKET-RAMJET HYBRID ENGINES

by Andrzej Dobrowolski

Lewis Research Center

Cleveland, Ohio

NATIONAL AERONAUTICS AND SPACE ADMINISTRATION • WASHINGTON, D. C. • OCTOBER 1966

ANALYSIS OF NONCONSTANT AREA COMBUSTION AND MIXING IN RAMJET AND ROCKET-RAMJET HYBRID ENGINES

By Andrzej Dobrowolski

Lewis Research Center
Cleveland, Ohio

NATIONAL AERONAUTICS AND SPACE ADMINISTRATION

For sale by the Clearinghouse for Federal Scientific and Technical Information
Springfield, Virginia 22151 – Price $2.00

ANALYSIS OF NONCONSTANT AREA COMBUSTION AND MIXING IN RAMJET AND ROCKET-RAMJET HYBRID ENGINES

by Andrzej Dobrowolski

Lewis Research Center

SUMMARY

A one-dimensional analysis of nonconstant area and nonconstant pressure burning and mixing processes is carried out using a prescribed pressure-area relation. The duct area ratio is advanced as an important parameter that affects the existence of flow solutions and the loss or buildup of the stagnation pressure ratio of the process. The critical condition of thermal choking associated with Mach number of unity for constant area duct is shown to assume other Mach values for various nonconstant area ducts. The concepts evolved are applied to idealized supersonic combustion ramjets and rocket-ramjet hybrid engines.

The nonconstant area combustion in a supersonic combustion ramjet results in a better specific impulse. Also, the separate mixing and burning, each with its appropriate duct configuration, leads to better performance than simultaneous mixing and burning in the case of the augmented rocket.

INTRODUCTION

The analysis of combustion or mixing processes in jet engines is usually confined to the cases of constant cross-sectional area or of constant gas pressure. References 1 to 3 are representative of the scope of the work in this field performed under the previously mentioned constraints. The present analysis is an attempt to treat the cases going beyond these confining stipulations. The burners and mixers thus evolved are applied to supersonic combustion ramjets and rocket-ramjet hybrid engines. In order to preserve the overall view of the processes involved, a one-dimensional treatment is carried out that assumes ideal gases with specific heats that do not change with temperature, no frictional penalties, and hydrogen stoichiometric burning in the primary or secondary flow. Complete mixing is assumed.

First, the supersonic burning is dealt with under the conditions of a variable geome-

try duct, and the requirements for its optimum performance are outlined. A critical condition, analogous to thermal choking at Mach 1 for the constant area duct, has to be recognized: this condition occurs at a Mach number that is not necessarily unity. The burning which takes place with its Mach number decreasing toward the critical is referred to as supercritical burning, while the burning which proceeds with its Mach number increasing toward the critical is referred to as subcritical burning. Thus, the concept of supersonic combustion may be replaced by the concept of supercritical combustion. There are also duct configurations where the Mach number hardly changes due to burning, however extensive this burning is.

Next the mixing is investigated by exploring (1) conditions for optimum buildup of the stagnation pressure of the secondary flow and (2) the option of a separate mixing and burning as compared to the simultaneous mixing with burning. The analyses are applied in the consideration of the performance of the ramjet and rocket-ramjet hybrid engines, and the ways of arriving at optimum duct configurations are illustrated. The appendix contains the derivation of pertinent equations.

SYMBOLS

A cross-sectional area of duct

$\bar{A}_1$ area ratio of secondary inlet over primary inlet, A_1/A_j

A^* duct area ratio, exit over inlet

C_F thrust coefficient, $\dfrac{\text{net thrust}}{(\text{dynamic pressure})(A_1 + A_j)}$

F function of Mach number, $M\sqrt{1 + \dfrac{\gamma - 1}{2} M^2}$

G function of Mach number and power index, $\epsilon + \gamma M^2$

G^* function of Mach number and power index, $G^* = \dfrac{G^{\epsilon(\gamma-1)/\gamma}}{X} = \dfrac{(\epsilon + \gamma M^2)^{\epsilon(\gamma-1)/\gamma}}{1 + \dfrac{\gamma - 1}{2} M^2}$

g dimensional constant, 32.2 (lb mass - ft)/(lb - sec^2)

h enthalpy, Btu/lb of gas

I_s specific impulse, sec

J mechanical equivalent of heat, 778 ft - lb mass/Btu

m mass flow per second, lb mass/sec

$\overline{m}_1$ entrainment ratio, m_1/m_j

M Mach number

N function of Mach number and power index, $\dfrac{M\sqrt{1 + \frac{\gamma - 1}{2} M^2}}{\epsilon + \gamma M^2}$

P pressure, lb/ft^2

q heat added, Btu/lb of air

R gas constant, ft-lb/(lb mass)(^oR)

S entropy, Btu/(lb)(^oR)

T absolute temperature, ^oR

X parameter, $1 + \frac{\gamma - 1}{2} M^2$

V velocity, ft/sec

α parameter, $\sin \alpha = N/N_c$

γ ratio of specific heats, C_p/C_u

Δ ratio of stagnation enthalpy of secondary flow h_1^o over stagnation enthalpy of primary flow h_j^o

ϵ power index in L. Crocco power area - pressure relation, $P_2/P_1 = (A_2/A_1)^{\epsilon/(1-\epsilon)}$

ρ density, (lb mass)/ft^3

Subscripts:

av average

b pertaining to burning

c value of function at critical point

j primary flow inlet

m end of mixing

0 referring to ambient conditions

1 secondary flow inlet

2 end of burning

3 end of nozzle expansion

Superscript:

o stagnation condition

PRESSURE - AREA RELATION

In solving the duct flow problems of heat addition or mixing, the one-dimensional treatment of the three conservative equations in their integrated form is found very useful for many flow regimes. A convenient assumption of the constancy of a certain quantity throughout the flow (e.g., the pressure or duct cross-sectional area) is commonly made. This permits the evaluation of the wall force integral in the momentum equation and hence the retention of the simple integrated form.

In order to enlarge the scope of the flow solutions, it would be desirable to have something else besides constant area or constant pressure cases. In general, there are many ways of expressing mathematically the variation of pressure with flow area. The one that has been chosen for this analysis because of its simplicity is due to L. Crocco (ref. 4) and is represented by

$$\frac{P}{P_1} = \left(\frac{A}{A_1}\right)^{\epsilon/(1-\epsilon)}$$

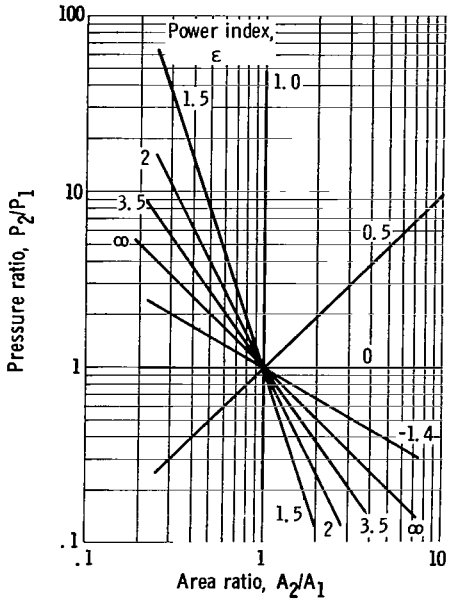

Figure 1. - Pressure-area relation, $\frac{P_2}{P_1} = \left(\frac{A_2}{A_1}\right)^{\epsilon/(1-\epsilon)}$

The pressure at any axial station is related to flow area through the single parameter ϵ. It is to be recognized that this arbitrary assumption as to the variation of the pressure inside the duct in no way conditions the length of the duct. Therefore, the area of the burner or mixer could be varied with length in such a manner that the existing finite rates of heat release or mixing yield the assumed variation of pressure with A. The convenience of this assumption becomes apparent not only by the ability to retain a simple integrated form but by the inclusion of constant pressure case with $\epsilon = 0$ and constant area case with $\epsilon = 1$. Thus, the introduction of the ϵ relation leads to some generalization and extension of the two more common cases.

Figure 1 presents the variation of the pressure ratio against the area ratio for several ϵ's. All pos-

sible variations are exhausted by positive and negative ϵ's.

It is of interest to study this generalized process in more detail - at first in combustion as an extrapolation of the known Rayleigh process and later on in mixing.

COMBUSTION

The process of heat addition to a flow in a duct of a constant cross-sectional area can be described in terms of the familiar Rayleigh curve in the h - S diagram shown below in sketch (a).

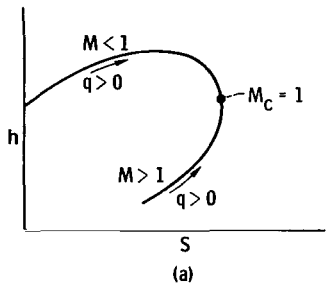

(a)

The extreme entropy point on the curve is a critical point depicting a thermal choking condition. The upper branch of the curve is associated with a subsonic flow, which with heat addition has its Mach number increasing, and the lower branch is associated with supersonic heat addition flow, with Mach number decreasing. The Mach number at the critical point is unity. Heat addition in excess of that required to achieve the critical or choking terminal Mach number will force an adjustment of the flow. The initial Mach number will be changed to a magnitude that is consistent with the amount of heat input.

It is fairly straightforward to show that the least stagnation pressure loss associated with a given amount of supersonic burning occurs in a process that reaches the critical condition.

Generalized Rayleigh Process

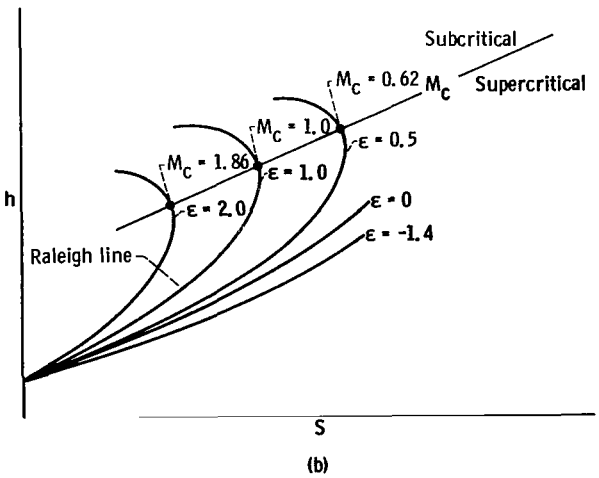

(b)

With the introduction of a nonconstant-area combustion process of the type specified by the Crocco ϵ relation, the enthalpy - entropy diagram assumes the form shown in sketch (b).

When one starts from the same initial value of the enthalpy, different ϵ's trace out different curvature lines. The upper branches of the lines delineate a subcritical process where Mach number increases (finally reaching the critical condition) because of heat addition, and the lower branches correspond to

a supercritical process where the Mach number is decreasing. One of the curves is the familiar Rayleigh line with $\epsilon = 1$. Again, it can be shown that the minimum stagnation pressure loss of the supercritical burning for fixed heat addition and ϵ occurs when the entrance M_1 is chosen such that the critical condition is reached at the end.

Critical Condition

To obtain a complete description of the flow at the exit section of the burner when the initial Mach number M_1, the initial stagnation enthalpy h_1^o, and the amount of heat added q are given, an energy balance equation is required which with the help of the other two conservation equations takes the form

$$\left(\frac{N_2}{N_1}\right)^2 = 1 + \frac{q}{h_1^o} \tag{7}$$

where

$$N = \frac{M\sqrt{1 + \frac{\gamma - 1}{2} M^2}}{\epsilon + \gamma M^2} \tag{6}$$

(The equations are described in the appendix. The equation numbers remain the same.) Equation (7) may be solved directly for M_2. When the function N is plotted against the Mach number M, figures 2(a) and (b) are obtained. In figure 2(a) for positive ϵ's, the highest points on the N curves define the critical conditions and result from the unique solutions to the previous heat addition equation. The critical Mach number is given by

$$M_c^2 = \left[\frac{\gamma}{\epsilon} - (\gamma - 1)\right]^{-1} \tag{8}$$

In the case of constant-area heat addition with $\epsilon = 1$, the critical Mach number is 1. For $\epsilon < 1$, this critical Mach number is subsonic, and for $\epsilon > 1$, the critical Mach number is supersonic. A positive ϵ varying from 0 to $\gamma/(\gamma - 1)$ exhausts all possible values for M_c from 0 to ∞. In general, for a given value of ϵ, two solutions or no solutions result as shown in sketch (c) when equation (7) is solved for M_2. Moderate heat addition at a given M_1 will yield subcritical and supercritical M_2 corresponding to a new N_2. At

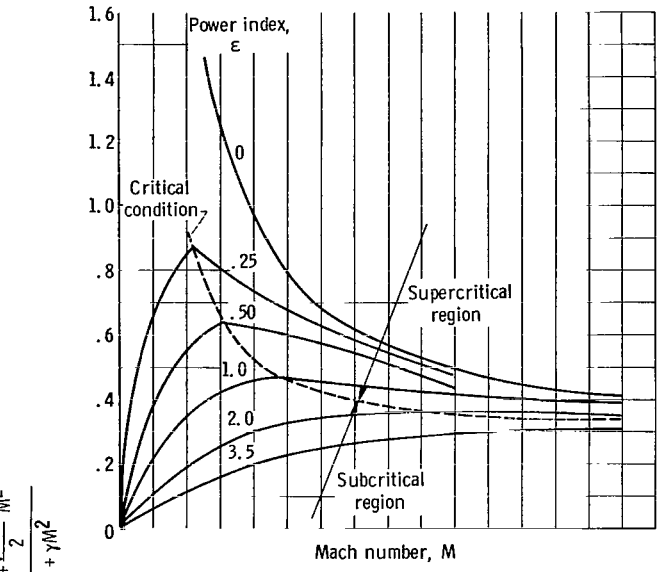

(a) Positive power index.

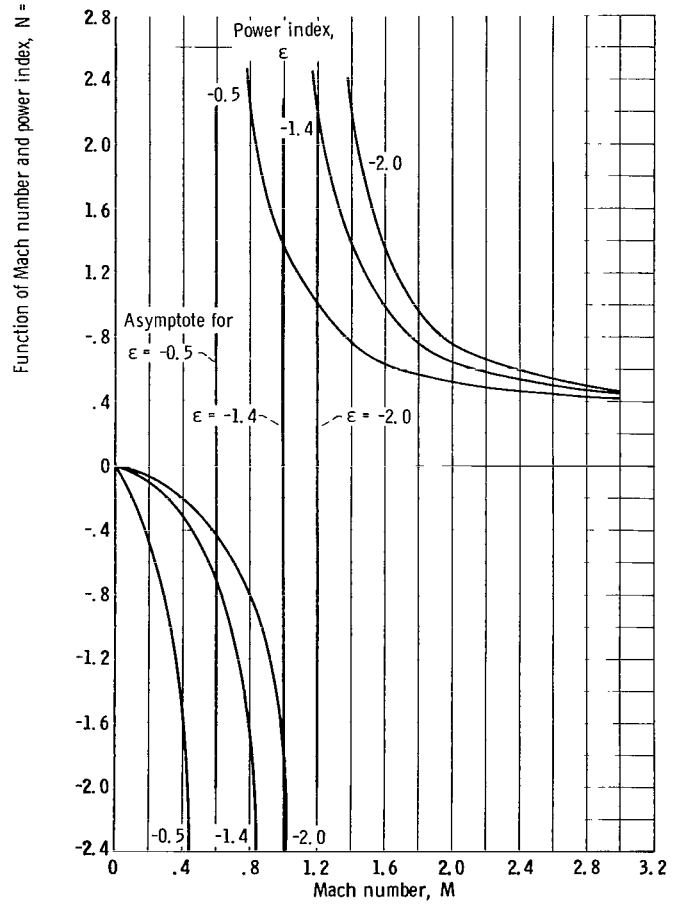

(b) Negative power index.

Function of Mach number and power index, $N = \frac{M\sqrt{1+\frac{\gamma-1}{2}M^2}}{\varepsilon+\gamma M^2}$

Figure 2. - Variation of N with Mach number.

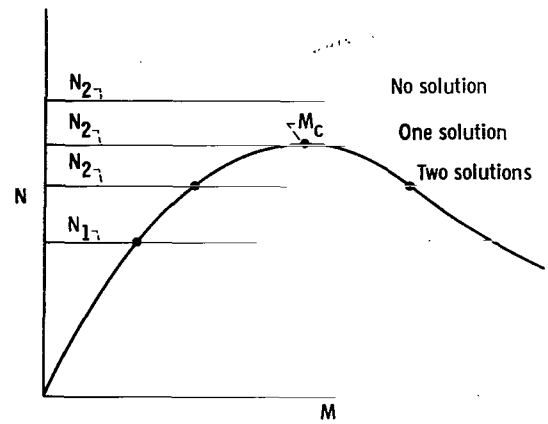

(c)

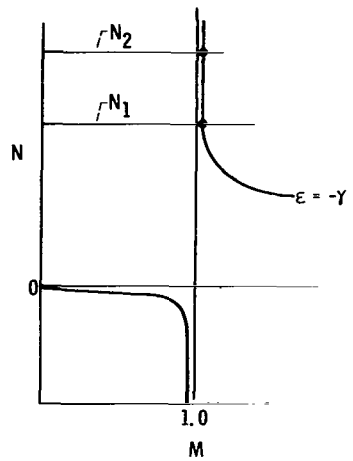

(d)

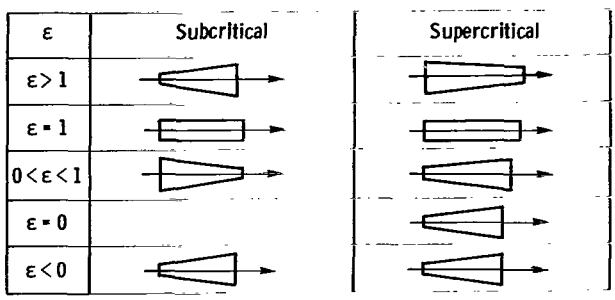

(e)

maximum heat addition, there is a single solution at a critical M_2. In the case of constant-area heat addition with $\epsilon = 1$, the one-solution situation corresponds to the thermally choked flow. Greater heat addition at a fixed M_1 yields cases where no solution (and hence no steady flow) is possible. In the case of $\epsilon = -\gamma$, the N curve increases rapidly in the neighborhood of $M = 1$, never quite reaching this asymptote. The maximum value of N_2 in this case is dictated by stoichiometric fuel addition which maximizes q and hence N_2/N_1 (see eq. (7)). This condition corresponds to a practically constant Mach number heat addition (see sketch (d)). The duct configuration is such that a flow at a Mach number approaching unity remains near unity after heat addition. From figure 2(b) it is seen that with a negative ϵ there is in general an asymptotic value of Mach number equal to $\sqrt{-\epsilon/\gamma}$ that the flow cannot quite reach; however, this Mach number can be approached as close as desired whether on the subcritical or the supercritical side. In sketch (e) the convergence or divergence of the duct is shown dependent on whether the flow is supercritical or subcritical and on the value of ϵ.

Stagnation Pressure Ratio

In order to be able to judge the merit of one particular ϵ (in other words, the advantage of one particular duct configuration for the given initial flow conditions) and one particular heat addition, the influence of ϵ on the stagnation pressure loss during burning has to be considered.

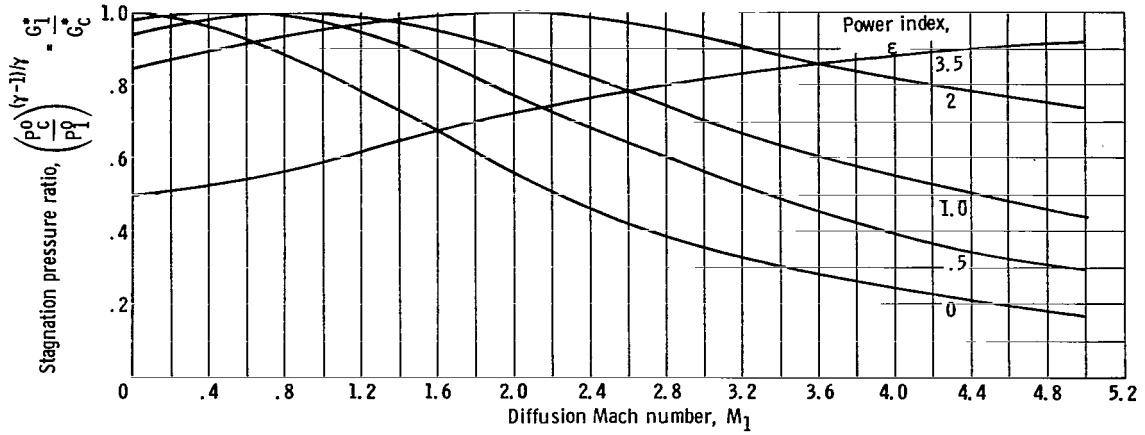

Figure 3. - Stagnation pressure ratio due to burning that changes flow from diffusion to critical Mach number.

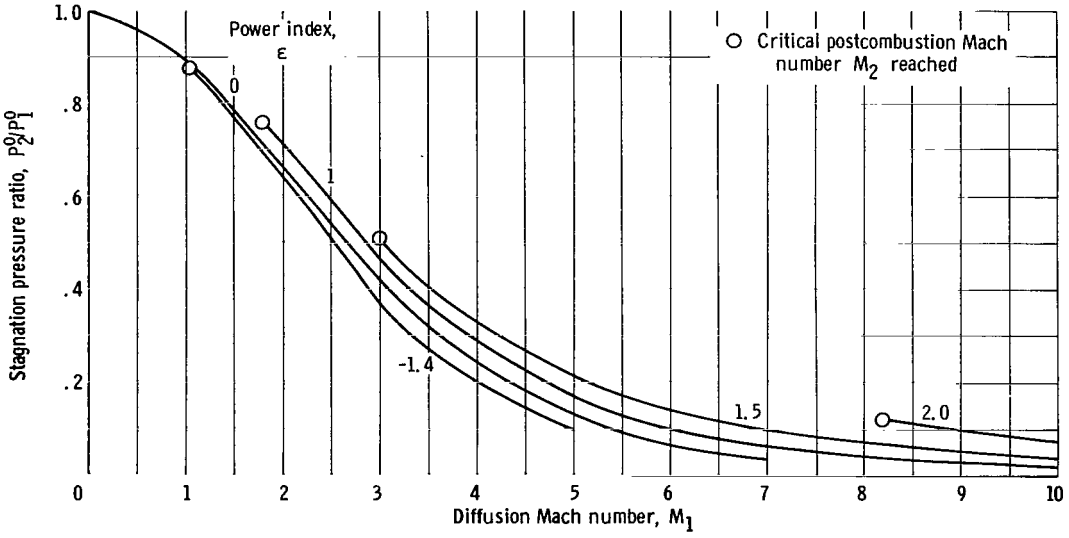

Figure 4. - Stoichiometric hydrogen combustion stagnation pressure ratio as function of diffusion Mach number for flight Mach number of 20.

Figure 3 shows the stagnation pressure ratio achieved during burning initiated at M_1 and ending at M_c. The stagnation pressure ratio of the process ending at any other Mach number is equal to the ratio of the pressure ratios corresponding to the initial and final Mach numbers since $\frac{P_2^o}{P_1^o} = \frac{P_c^o}{P_1^o} \Big/ \frac{P_c^o}{P_2^o}$. The relation between M_1 and M_2 is found by applying the N expression of the preceding section for a particular inlet stagnation enthalpy (function of flight Mach number) and heat addition (function of fuel type and fuel-air ratio). Figure 4 shows the stagnation pressure ratio for several ϵ values and supercritical burning for the specific case of flight Mach number $M_0 = 20$ and stoichiometric combustion of hydrogen. It is seen that given a series of ϵ ducts with the supercritical flows at the

same initial Mach number M_1 and subjected to the same heat addition, the larger the ϵ, the smaller will be the stagnation pressure loss. From sketch (e), where the shapes of the ducts are noted, this would imply, for example, that a convergent duct is superior to a constant area duct for the same M_1.

Given a series of ϵ ducts with the supercritical flows of the same stagnation enthalpy at different initial Mach numbers M_1, such that each duct reaches a critical condition after the same heat addition, the larger the positive ϵ, the larger will be the stagnation pressure loss (circled points in fig. 4). This implies that a constant area duct is superior to a convergent duct if a critical condition is reached in both ducts. (The shapes of duct are noted from sketch (e).) Thus diffusing (without losses) the flow sufficiently for the subsequent heat addition in the constant area duct to reach a critical condition will yield a better stagnation pressure ratio than direct use of a critically convergent duct. A diverging, critical, constant Mach number duct ($\epsilon = -1.4$) is still better. Best of all is the constant pressure case ($\epsilon = 0$); however, heat addition in this case requires the flow to pass smoothly from supersonic to subsonic. This condition may not be achievable in practice.

In general, the critical ϵ for any given M_1, for a given heat addition, and for initial stagnation enthalpy, that secures the attainment of the critical endpoint, can readily be identified by a direct calculation as derived in the appendix (see eq. (15)).

Optimization of Inlet-Combustor Combination

In the design of an inlet-burner combination, the choice of ϵ for the burner duct and the diffusion Mach number M_1 will reflect directly on the overall stagnation pressure loss. For every ϵ it is seen that the lowest permissible M_1 minimizes the stagnation pressure loss due to heat addition. However, diffusion to low values of M_1 generally causes greater pressure losses in the inlet diffuser. Selection of the optimum ϵ and M_1 must hence consider the combined inlet and combustor.

The performance of a supersonic combustion ramjet inlet is a function of the inlet type, the flight Mach number M_0, and the design diffusion Mach number M_1. For illustrative purposes, figure 5 shows the pressure recovery of a representative supersonic combustion ramjet inlet. It is based on the evaluation of the stagnation pressure of the flow following three oblique shocks of equal static pressure rise.

If one has an inlet whose performance is a function of the diffusion Mach number M_1 and a burner with a specific ϵ, where the stagnation pressure ratio achieved is a function of M_1, it is an easy matter for a given flight condition and heat addition to search and find an M_1 that will result in an overall minimum stagnation pressure loss.

Generally, the critical condition for burning is not reached. Diffusing the inducted flow of air to a very low Mach number M_1 incurs a heavy penalty in stagnation pressure

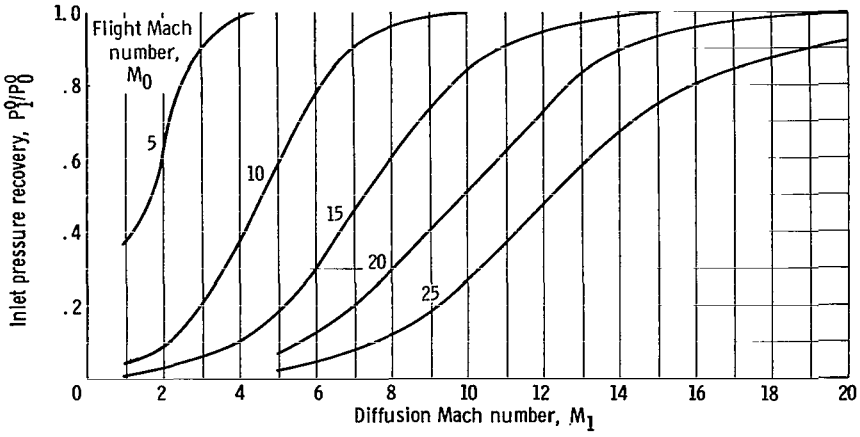

Figure 5. - Inlet pressure recovery of a representative supersonic combustion ramjet for three oblique shocks of equal strength.

recovery; however, this makes it possible for the burning to take place near the critical point with its favorable stagnation pressure ratio. On the other hand, hardly diffusing the oncoming flow, and thus allowing a high pressure recovery, compromises the stagnation pressure ratio of combustion that of necessity occurs far off the critical point. Somewhere in between those two extreme conditions an optimum is usually found.

If one uses the inlet data of figure 5 and the combustor data of figure 4, from which the stagnation pressure variation of hydrogen stoichiometric burning against M_1 can be found, the effect of M_1 on the overall pressure ratio can be shown as in figure 6 for $M_0 = 20$ and a range of ϵ.

It is seen that the maximum stagnation pressure is reached for $\epsilon = 2.0$ and $M_1 = 8.2$ under the condition of critical burning. Figure 7 shows the variations of the postcombustion Mach number M_2 against the diffusion Mach number M_1. The postcombustion M_2 hardly changes at large diffusion Mach numbers.

Repeating the same procedure for a series of flight Mach numbers gives figure 8, where the optimum diffusion Mach numbers are noted. The signficance of the maximization of the stagnation pressure ratios product for the evaluation of the optimum specific impulse is seen from equations (12) and (13) in the appendix. The specific impulse evaluated at the ascertained M_1's and ϵ's, which change with M_0, is shown in figure 9 for the M_0 range of 10 to 25. This is compared with the performance of the constant ϵ engines. It is seen that modest, but significant, improvements are offered by the optimum-ϵ case as compared to the constant-area case. It is noted that the improvement would be magnified had a less idealized expansion nozzle been assumed.

The ϵ of the optimum variable ϵ ramjet is seen to vary from $\epsilon = 0.5$ at $M_0 = 10$ to $\epsilon > 2$ at $M_0 = 25$. Figure 10 describes in detail the ϵ and the associated area ratio variation of the optimum ramjet for the assumed conditions. From a divergent burner duct at lower Mach numbers M_0, the specified duct shape changes to a constant

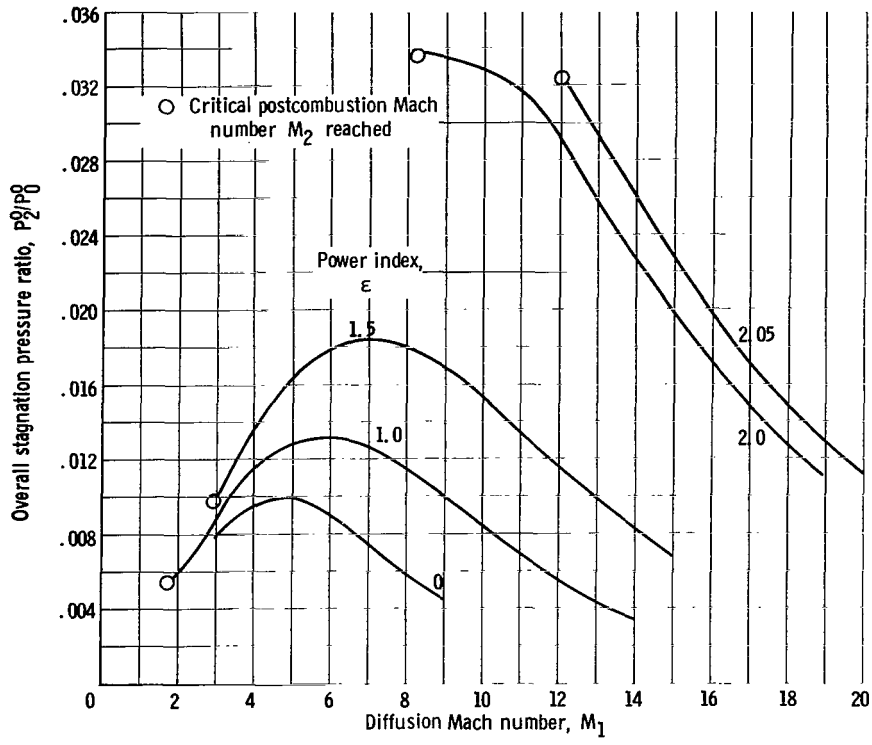

Figure 6. - Overall stagnation pressure ratio due to induction and combustion (hydrogen stoichiometric) for flight Mach number of 20.

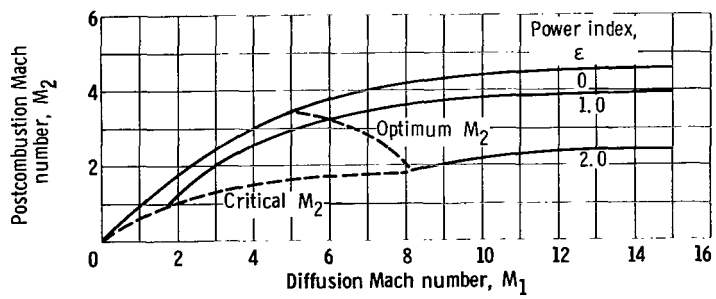

Figure 7. - Postcombustion Mach number as function of diffusion Mach number for flight Mach number of 20.

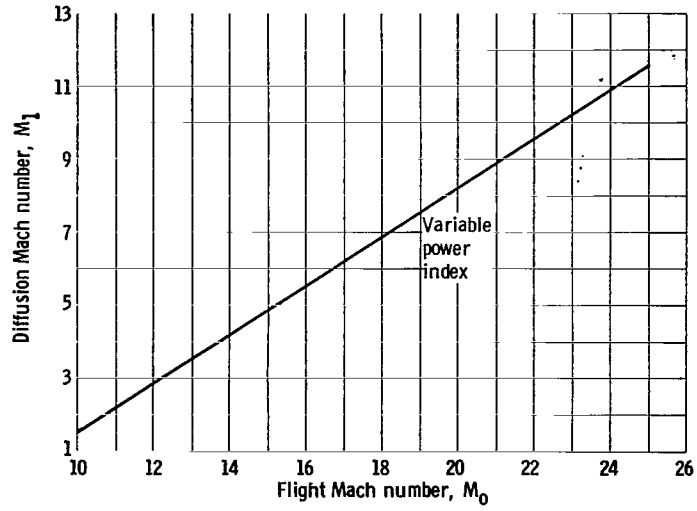

Figure 8. - Diffusion Mach number as function of flight Mach number.

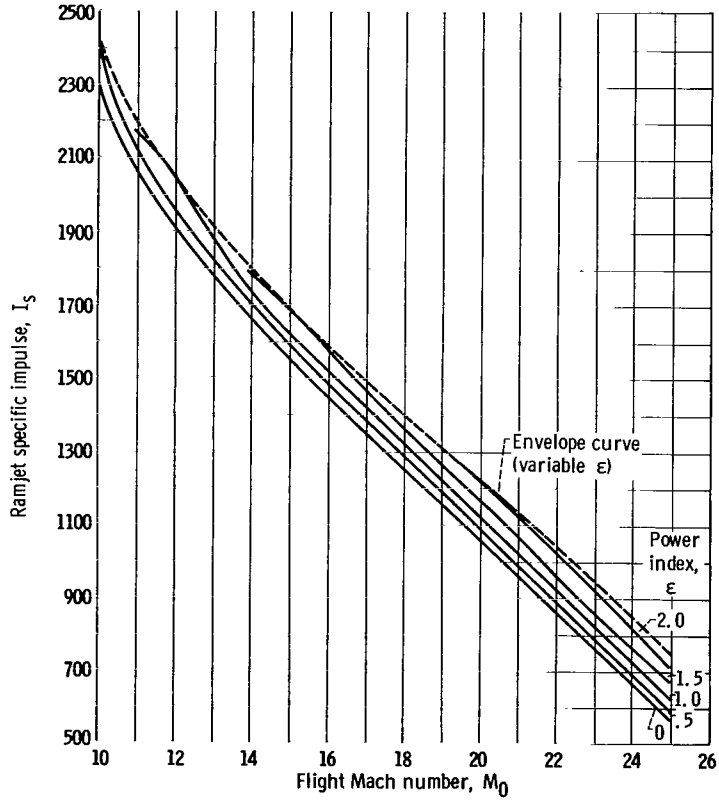

Figure 9. - Ramjet specific impulse as function of flight Mach number. Hydrogen stoichiometric combustion; full expansion into ambient conditions.

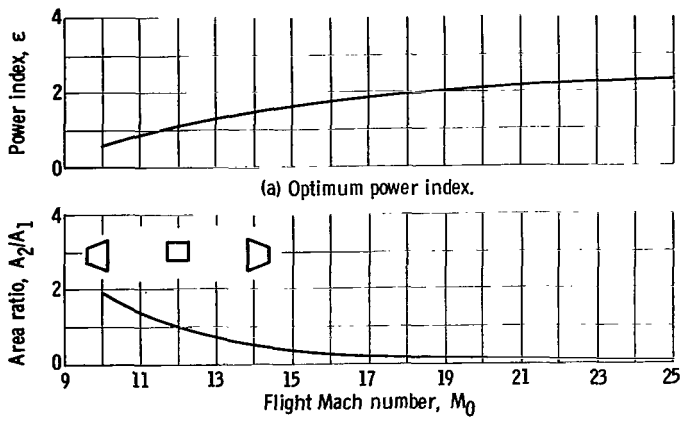

(a) Optimum power index.

(b) Burner exit area to inlet area ratio.

Figure 10. - Supercritical ramjet.

area and later to a convergent one at higher flight Mach numbers.

The indicated desirability of employing a convergent combustor at high flight Mach numbers should be tempered by the following realization: as previously pointed out (fig. 4), best combustion performance is obtained if the Mach number entering the combustor is near unity and heat is then added with an ϵ of 1 or less (corresponding to constant area or diverging area ducts), since this yields an exit Mach number near unity. However, diffusing to such a low M_1 causes excessive inlet losses according to the assumed schedule of figure 5, so that the optimum M_1 is considerably higher. In order to retain the benefit of a low exit Mach number, the calculations then indicate the use of a converging duct (provided by a high ϵ). The duct thus performs the function of a diffuser, but without the pressure losses associated with the assumed inlet (since the present calculations consider combustor stagnation pressure losses that arise from heat addition only, no losses due to area changes as such are included).

A more realistic inlet model than that of figure 5 would recognize the possibility of substantial internal contraction, yielding low M_1, with little loss in pressure recovery. In this situation, it is possible that high ϵ's and converging combustors would not appear desirable.

MIXING

The preceding section considered the problem of heat addition to a single supersonic flow through a nonconstant area duct with applications to the supersonic combustion ramjet. The problem now considered is one of mixing two streams in a nonconstant area duct. This applies, for example, to submerging the exhaust of a rocket in a secondary flow of air in a ducted rocket arrangement, which results in an increase of specific impulse due to an exchange of thermal and mechanical energy. A further benefit may be obtained by a subsequent addition of heat to the mixed flow.

The algebraic treatment of the three conservation equations, in their integrated form for the two flows undergoing complete mixing, leads to complex expressions for the relations between certain variables of interest because of the existence of so many parameters. One of the more tangible relations of mixing two flows is the change of magni-

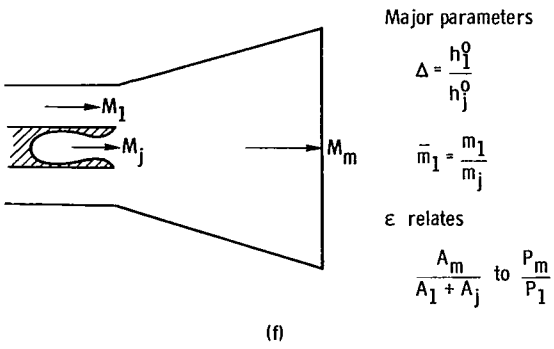

(f)

tude of the Mach number of the resultant mixed flow M_m, which is due to the changes of the secondary flow initial Mach number M_1 (see sketch (f)). Once the character of those variations of M_m and the bounds on M_1 for the existence of solutions that circumscribe the regions of interest have been ascertained, it is of prime concern to seek to achieve as high a stagnation pressure buildup in the mixed flow as possible in those regions of validity.

Bounds on the Solutions

With a fixed primary flow, the relation between M_m and M_1 will depend on the mass ratio $\bar{m}_1$, the stagnation enthalpies ratio Δ, the static pressure ratio P_1/P_j, and the power index ϵ when perfect mixing is assumed (see eq. (30) in the appendix). It is of interest to first examine how the value of M_1 influences the solution for M_m.

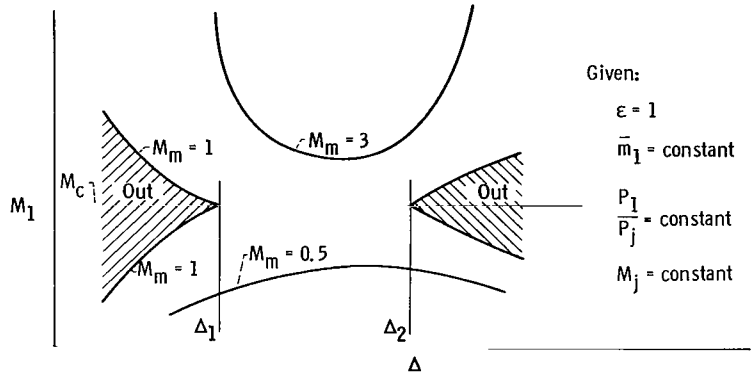

(g)

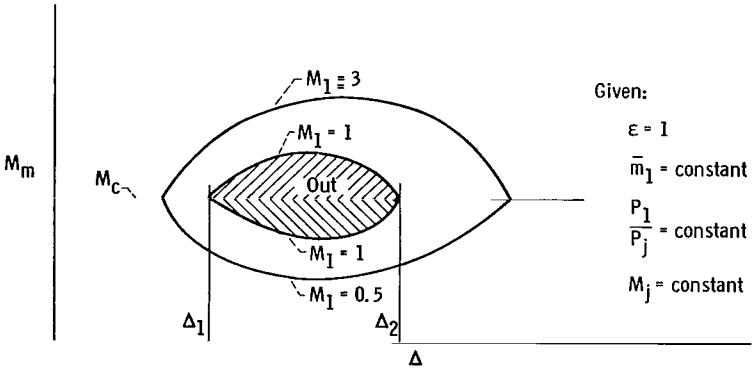

(h)

Sketches (g) and (h) classify the interdependence of M_m, M, and Δ for a specific case of $\epsilon = 1$. The three regions of the diagrams correspond to three ranges (low, medium, and high) of values for the stagnation enthalpy ratio Δ. In sketch (g), for the low and high ranges of Δ, the shaded regions denote the values of M_1 for which there are no solutions for M_m. Above this shaded region, values of M_1 result in an M_m that is greater than M_c, while along the curves separating the two regions the values of M_1 result in an M_m that is equal to M_c. Below the shaded regions, values of M_1 result in an M_m which is less than M_c, and again the bounding curve denotes values of M_1 that result in an M_m equal to M_c. For the low range of Δ, as Δ increases the excluded range of M_1 decreases, and finally vanishes at a point $M_1 = M_m = M_c$. In sketch (h) it is seen that above the shaded region values of M_m correspond to values of M_1 which are greater than M_c, while below the shaded region values of M_m correspond to values of M_1 which are less than M_c. The lines bounding the shaded region denote values of M_m for which M_1 is equal to M_c. The excluded region occupies the medium range of Δ.

The situation can be elucidated further by the familiar N function consideration as shown in sketch (i). The relation between N_1 and N_m in terms of $\overline{m}_1$ and Δ has to be solved to obtain M_m. The shaded portions of the curve for N_1 will produce various values for M_m until the limiting M_1 values are reached, which results in M_m at the critical value. A value of M_1 between the limiting points will produce no solution. This situation corresponds to the low range of Δ in sketch (g).

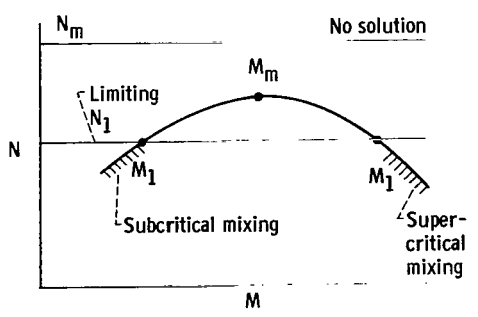

(i)

From a return to sketch (h) and an observation of the medium magnitude of Δ, it is noticed that a large region of M_m values is excluded. This means that whatever value for M_1 is prescribed, M_m cannot assume a large spectrum of values. The corresponding N function is shown in sketch (j).

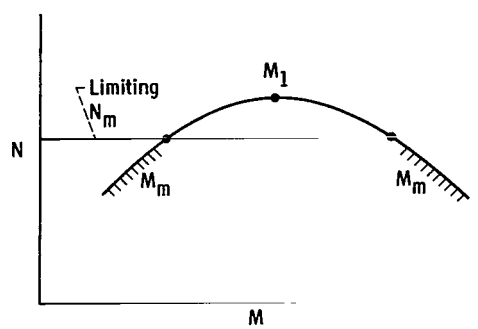

(j)

Regardless of the value of M_1, M_m can be found only along the shaded portions of the curve. The critical value for M_1 results in limiting M_m's.

It becomes obvious from the previous discussion that the diffusion Mach number M_1 delivered by the inlet into the mixer is of critical importance, once exit conditions have been prescribed, since certain regions are excluded. Therefore, careful analysis

must be done for a fixed configuration flying a changing flight path.

In order to evaluate overall engine performance, the stagnation pressure buildup achieved during mixing and its dependence on M_1 must be considered.

Stagnation Pressure Ratio

With a fixed primary flow, the stagnation pressure ratio of the mixed flow, besides depending in large measure on the secondary flow Mach number M_1, will depend also on the mass ratio $\bar{m}_1$, stagnation enthalpy ratio Δ, and ϵ (eq. (35) in the appendix). A typical graphical representation of the stagnation pressure ratio P_m^o/P_1^o variation against M_1 for fixed values of the rest of the parameters is shown in sketch (k).

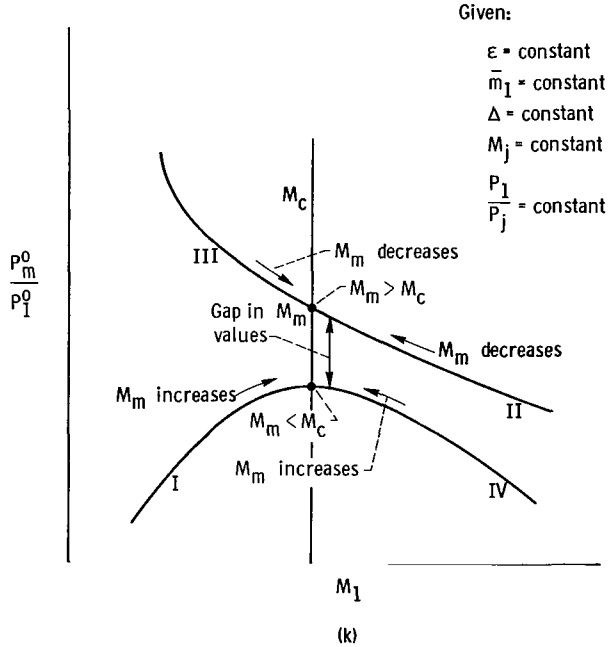

(k)

The existence of two distinct curves is explained by the duality of the solution for the mixed flow Mach number M_m, which is obtained through the evaluation of the N function. The situation corresponds to the shaded region of sketch (h).

The two parts of sketch (ℓ) show the solutions with their associated branches of the curves. These selected values for M_m, like I and II that occur on the same sides of the curves as the given M_1, are referred to as the regular solutions. The two on the other sides of the curves will be called crossover solutions. In the familiar constant-area duct cases ($\epsilon = 1$), where only a subsonic M_1 is allowed, the solution I is elaborated and the solution III, called a supersonic one, is often disregarded.

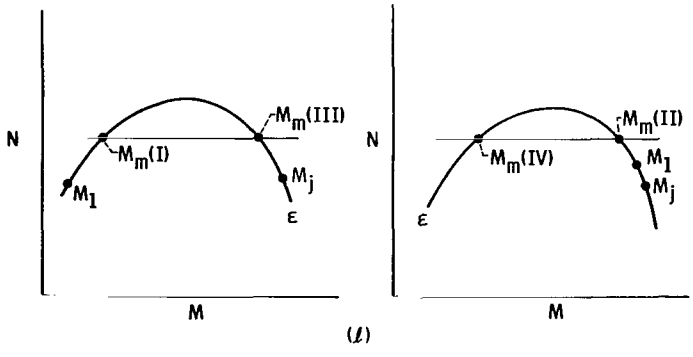

(ℓ)

A somewhat different stagnation pressure ratio diagram (shown in sketch (m)) may be arrived at by recollection of the remarks made concerning the existence of the bounds

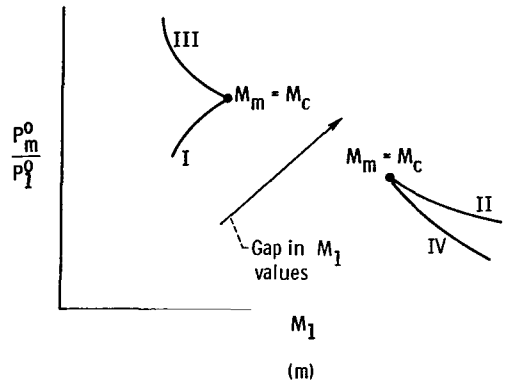

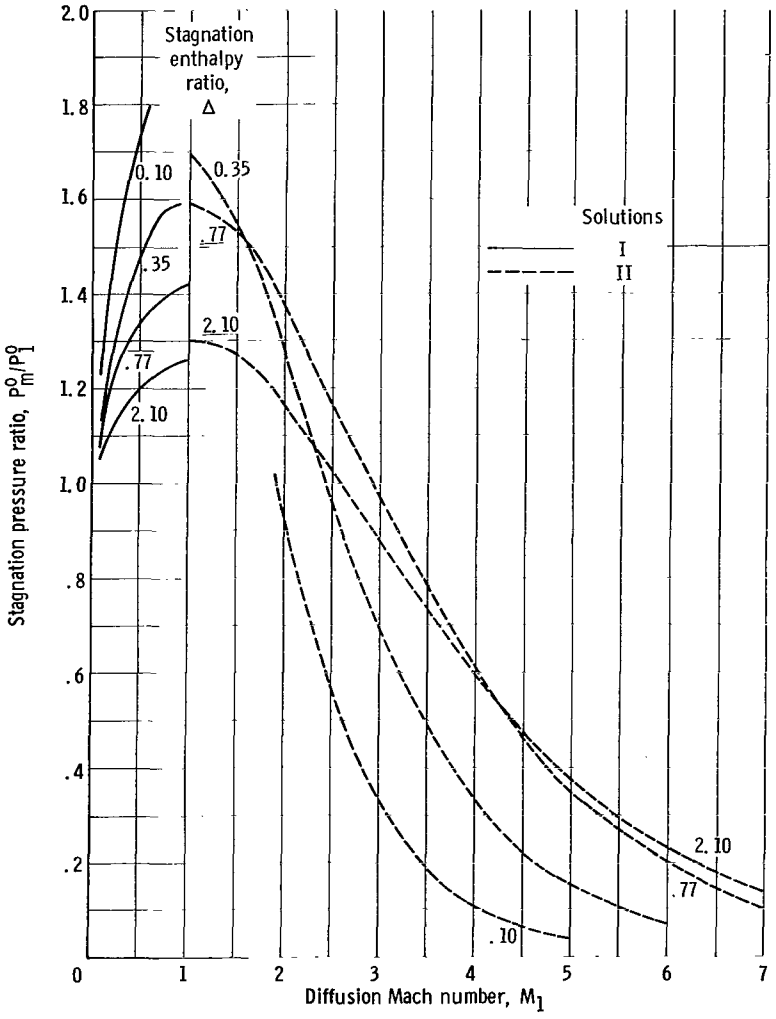

Figure 11. - Regular solutions (I and II) for stagnation pressure ratio at various stagnation enthalpy ratios. Mass ratio, 3; power index, 1.0; static pressure ratio, $P_1/P_j = 1$. (See sketch (h) for explanation of gap in curve at $\Delta = 0.10$.)

on the solutions for the mixed flow. A spectrum of values of M_1 does not give any solution for the mixed flow. This corresponds to the situation in sketch (g) (the shaded regions). In figure 11 the regular solutions (I and II) for the stagnation pressure ratio at various Δ's have been plotted against M_1 for $\overline{m}_1 = 3$ and $\epsilon = 1.0$. The opposite effects of Δ in subcritical and supercritical mixing are noticed. The gap in the curve for $\Delta = 0.10$ corresponds to the shaded region of sketch (g).

It is seen that the selection of M_1 is of crucial importance for the performance of the mixer, with the value of M_1 nearest to unity always yielding the best stagnation pressure ratio.

Figure 12 shows the variation of the stagnation pressure ratio of the solutions at constant M_1 and Δ against ϵ. The mild increase of the parameter with the increase of ϵ is observed. Finally, in figure 13 the dependence of the maximum obtainable stagnation pressure ratio on the mass ratio is found. As to be expected, the smaller the amount of low-energy secondary air, the greater the increase in its stagnation pressure.

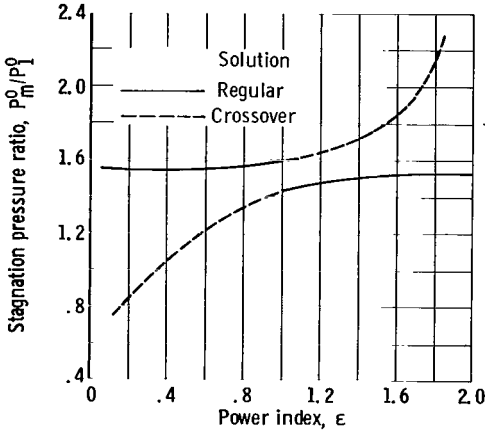

Figure 12. - Variation of stagnation pressure ratio with power index. Mass ratio, 3; diffusion Mach number, 1.0; stagnation enthalpy ratio, $\Delta = 0.77$.

Mixing and Burning

Higher specific impulses may be possible if the function of momentum transfer mixing is separated from the function of combustion by provision of two separate chambers in the duct, one being the mixer and the other being the burner. Beside the advantage due to heat addition taking place at elevated pressure,

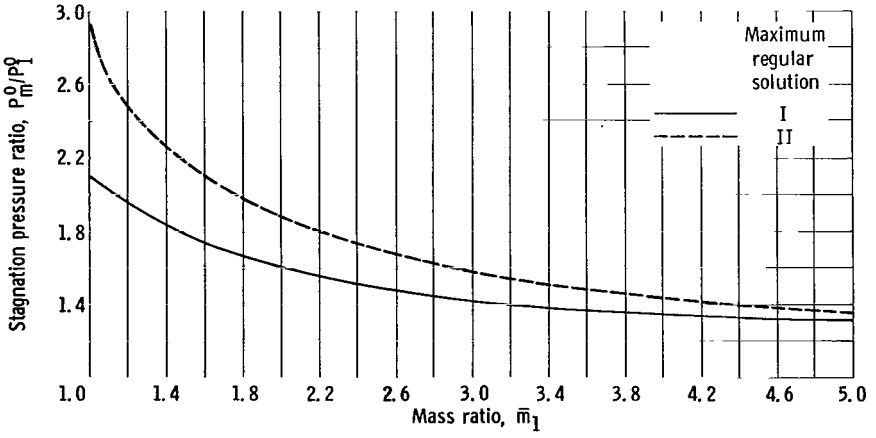

Figure 13. - Dependence of maximum stagnation pressure ratio on mass ratio. Power index, 1; stagnation enthalpy ratio, $\Delta = 0.77$.

another advantage is the opening of scope for the greatest possible stagnation pressure buildup in the mixer and the least possible loss of it in the burner, or an optimum compromise for the maximization of the product. It may be expected that the two separate chambers, each with its own optimum geometry (in other words, two in number geometries), show a drastic improvement over the constraint of one single geometry associated with a single-chamber concept.

Ideally, the gross jet thrust per unit of primary mass flow of the engine is given by

$$(\overline{m}_1 + 1)V_3 = (2gJ)^{1/2}(1 + \overline{m}_1)\left(h_1^o + q + \frac{h_j^o - h_1^o - q}{1 + \overline{m}_1}\right)^{1/2}\left[1 - \left(\frac{P_0}{P_3^o}\right)^{(\gamma-1)/\gamma}\right]^{1/2} \qquad (40)$$

whether it is one- or two-chamber variant.

The difference will be in the value of the stagnation enthalpy of primary jet h_j^o, which in the case of the single-chamber case will be quite smaller for limited oxidizer-fuel ratios. With the single chamber, the oxidizer-fuel ratio of the primary jet is below the stoichiometric ratio, thus yielding a comparatively small h_j^o. It is assumed that the fuel-rich primary is the only source of fuel for the secondary flow.

As to the pressure term, what remains to be mentioned is the comparative difficulty of optimizing it in the single-chamber concept. Sketch (n) shows the typical relation between M_m and M_1 plotted against Δ for the single chamber. Large exclusion areas are noted. A large spectrum of M_1 values produces no solution.

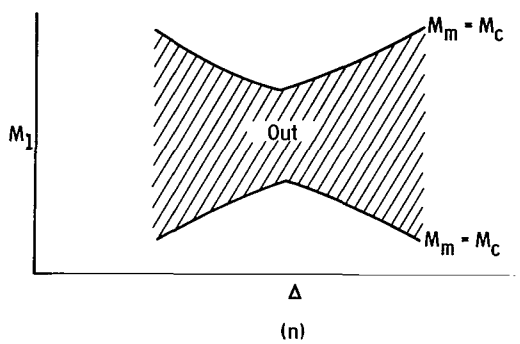

(n)

To compare conclusively the virtues of "mixing followed by burning" to "mixing while burning," an examination of the corresponding stagnation pressure ratios is in order.

For every diffusion Mach number M_1 and a given stagnation enthalpy ratio Δ, the performance of the optimum ϵ mixer duct configuration coupled to an optimum supercritical burner (which as seen previously must be a critical ϵ duct) is juxtaposed with the optimum mixer burner in figure 14. A marked difference is noted. The gap in the lower curve is explained by the lack of the solutions for a spectrum of M_1, as shown in sketch (n). A significant advantage in magnitude of the stagnation pressure and in the range of its achievable conditions is seen in the case of separate mixing and burning. This advantage prevails in most of the cases.

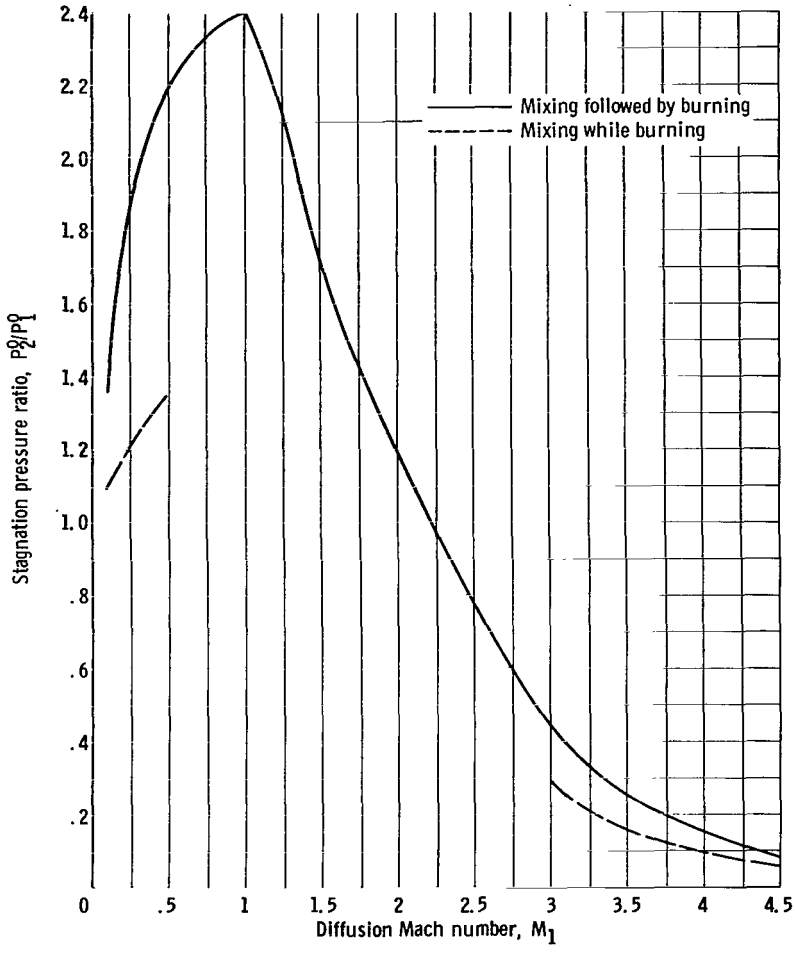

Figure 14. - Stagnation pressure ratios for "mixing followed by burning" and "mixing while burning". Mass ratio, 1; power index of mixing duct, 1.0; flight Mach number, 10.

TYPICAL ENGINE PERFORMANCE

The separate mixer and burner systems need more examination in terms of the overall performance that includes an inlet and a nozzle.

If for the nozzle a full expansion to the ambient pressure and a given mass ratio $\overline{m}_1$ for the whole engine are assumed, it is necessary to correlate the three stagnation pressure ratios achieved in induction, mixing, and stoichiometric hydrogen burning at any flight Mach number M_0.

As seen in figure 5 (p. 11) the stagnation pressure ratio of induction is related directly to the diffusion Mach number M_1. This variable in turn, as it has been seen in figure 11 (p. 18), affects the stagnation pressure ratio of mixing.

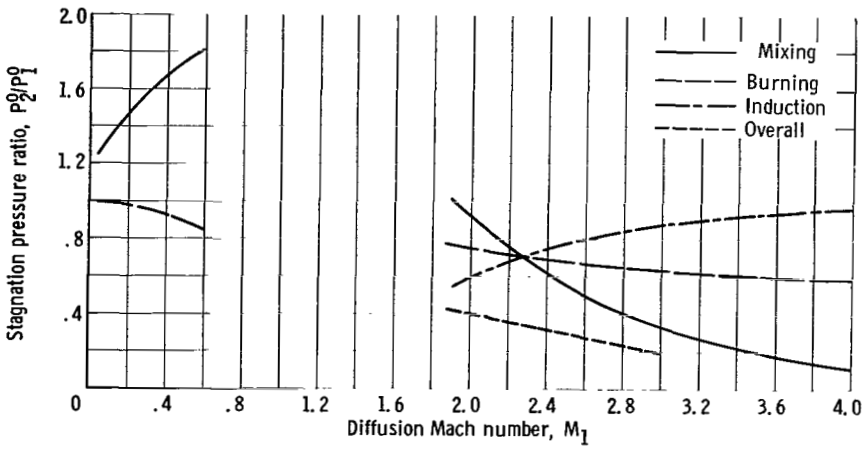

Figure 15. - Stagnation pressure ratios of induction, mixing, and burning. Mass ratio, 3.0; power index of mixing duct, 1.0; power index of burner, critical; flight Mach number, 5; separate mixing and burning.

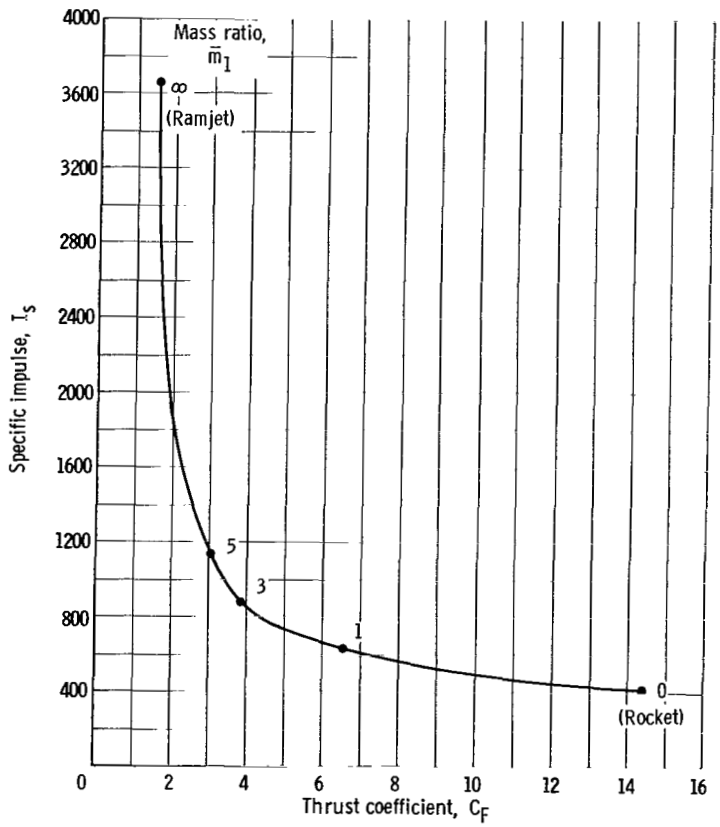

Figure 16. - Variation of specific impulse with thrust coefficient. Flight Mach number, 5; altitude, 70 000 feet.

In figure 15, the stagnation pressure ratios of induction, mixing, and burning for the case of $M_0 = 5$ and $\overline{m}_1 = 3$ are plotted against the diffusion Mach number M_1 for a single ϵ of mixing duct $\epsilon_m = 1$. The primary jet is a stoichiometrically burnt hydrogen in oxygen, and the static-pressures ratio P_i/P_j is unity. Whatever the resultant mixing Mach number M_m, the critical burning follows, and its stagnation pressure ratio is also shown in figure 15. Repetition of the same procedure for several ϵ_m leads to the best obtainable overall pressure ratio that can be obtained for the selected case.

Relative to its specific impulse and its thrust coefficient, the hybrid engine considered occupies an intermediate position between pure ramjet and a rocket. The ramjet has a high specific impulse but a relatively low thrust-to-weight ratio, and the chemical rocket has substantially opposite characteristics. Where exactly a given hybrid engine is located in the wide spectrum of both mentioned parameters ought to be implied by the entrainment ratio.

This spectrum, delineated by the ramjet and the rocket at both extremes, is shown in figure 16, where the specific impulse is plotted against the thrust coefficient for the flight Mach number $M_0 = 5$ and the altitude of 70 000 feet. There is an order-of-magnitude variation in both propulsion characteristics, and the actual choice of the operating point will ensue from the integration of the propulsion and the vehicle for any particular mission.

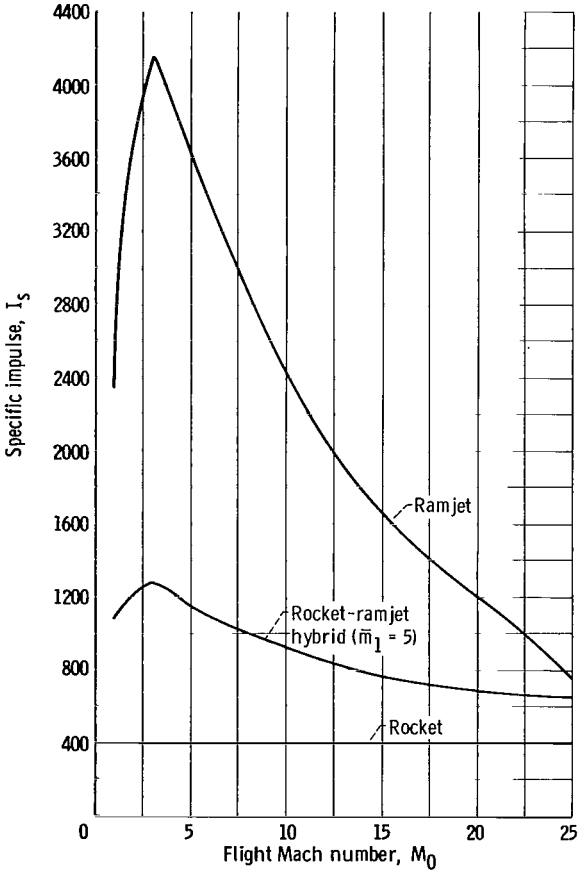

Figure 17. - Variation of specific impulses with flight Mach number.

In order to have some insight into the performance capability of a booster with a rocket-ramjet propulsion, the specific impulse of the engines against the flight Mach number has been plotted in figure 17. The area enclosed by the curves of the ramjet and the rocket maps out the capability of the hybrid engines. One of those engines with an entrainment ratio $\overline{m}_1 = 5$, whose vehicle trajectory is shown in figure 18, has been plotted. Its performance has been optimized at every flight Mach number by the method shown earlier for $M_0 = 5$. Figure 19 shows the variation of some important parameters of this particular hybrid engine. It is seen that a great measure of flexibility would be required from the mixer and the burner.

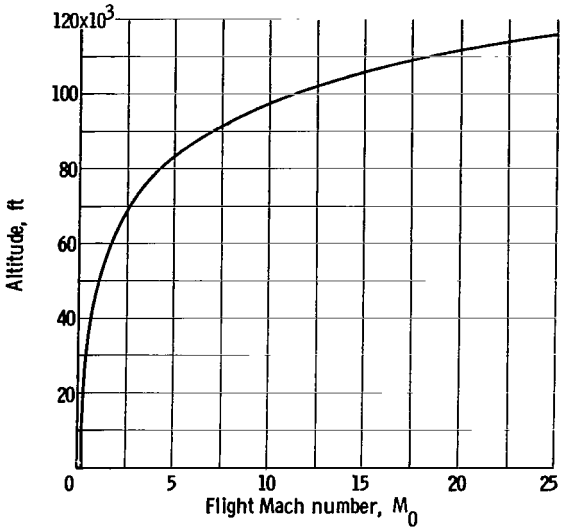

Figure 18. - Flight path of rocket-ramjet hybrid.

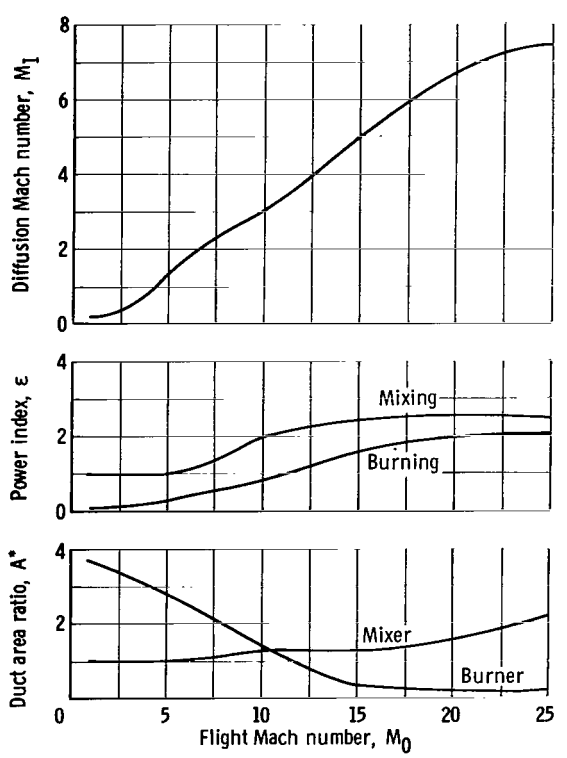

Figure 19. - Variation of important rocket-ramjet parameters with flight Mach number.

CONCLUDING REMARKS

Based on the assumption of certain idealized conditions, the analysis of nonconstant area combustion and mixing has been carried out. The results of this analysis indicate that the duct shape is an important consideration in the evaluation of the performance of the burner or the mixer. The area ratio as a variable, besides broadening the scope of the possible flow solutions, leads to the choice of a suitable and optimum duct for any boundary conditions.

Special attention has to be given to the magnitude of the diffusion Mach number of the secondary flow duct entrance. This Mach number affects greatly the performance of the duct.

The nonconstant area combustion in a supersonic combustion ramjet results in a better specific impulse. Also, if the separation is feasible, the separate mixing and burning, each with its appropriate duct configuration, leads to better performance than simultaneous mixing and burning in the case of the augmented rocket.

Admittedly, the varying flight conditions could in general demand a varying configuration or many different fixed configurations. One of those configurations, however, will do better for the whole flight spectrum than the rest of them; thus, a fixed-geometry engine design is not precluded. The best geometry can be ascertained by the derived methods of this report. In general, the insight into nonconstant area processes afforded by this report should be helpful in the design of actual engines.

Lewis Research Center,
National Aeronautics and Space Administration,
Cleveland, Ohio, June 3, 1966,
126-15-09-08-22.

APPENDIX - EQUATIONS OF BURNING AND MIXING

Various relations are derived, starting with the standard one-dimensional treatment of the three conservation equations as modified by Crocco's device for the use of single-flow heating.

Heat Addition to a Single Flow

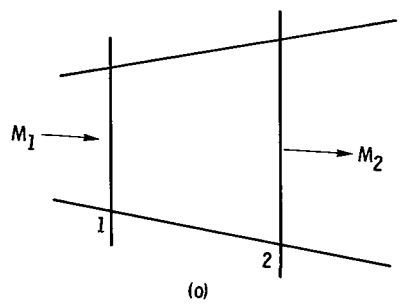

(o)

The conservation of mass equation is (see sketch (o))

$$m_1 = m_2 \tag{1}$$

or since

$$m = \rho AV = \frac{PAM}{RT}\sqrt{g\gamma RT} = \frac{PAM\sqrt{\gamma g}}{\sqrt{RT}} = \frac{PA\gamma F\sqrt{g}}{\sqrt{\gamma RT^o}}$$

where

$$F = M\sqrt{1 + \frac{\gamma - 1}{2}M^2}$$

it will assume the form

$$\frac{P_1A_1F_1}{\sqrt{T_1^o}} = \frac{P_2A_2F_2}{\sqrt{T_2^o}} \tag{2}$$

if $\gamma_1 = \gamma_2$

From the conservation of momentum,

$$\frac{1}{g}(m_2V_2 - m_1V_1) = P_1A_1 - P_2A_2 + \int_1^2 P\,dA \tag{3}$$

If it is assumed that the Crocco relation holds,

$$\frac{P}{P_1} = \left(\frac{A}{A_1}\right)^{\epsilon/(1-\epsilon)}$$

then

$$\int_1^2 P\, dA = \int_1^2 P_1\left(\frac{A}{A_1}\right)^{\epsilon/(1-\epsilon)} dA = (1 - \epsilon)\,(P_2A_2 - P_1A_1)$$

Substituting this into equation (3) gives

$$\frac{m_2V_2}{g} + \epsilon P_2A_2 = \frac{m_1V_1}{g} + \epsilon P_1A_1$$

Since

$$V = M\sqrt{g\gamma RT}$$

and

$$m = \frac{PAM\gamma\sqrt{g}}{\sqrt{\gamma RT}}$$

the equation can be transformed into

$$P_2A_2\left(\epsilon + \gamma_2M_2^2\right) = P_1A_1\left(\epsilon + \gamma_1M_1^2\right)$$

or

$$P_2A_2G_2 = P_1A_1G_1 \qquad (4)$$

where

$$G = \epsilon + \gamma M^2$$

The conservation of energy equation is

$$h_1^o + q = h_2^o \tag{5}$$

In equation (2) F can be replaced by GN where

$$N = \frac{F}{G} = \frac{M\sqrt{1 + \frac{\gamma - 1}{2} M^2}}{\epsilon + \gamma M^2} \tag{6}$$

Then

$$\frac{P_1 A_1 G_1 N_1}{\sqrt{T_1^o}} = \frac{P_2 A_2 G_2 N_2}{\sqrt{T_2^o}}$$

which on account of equation (4) becomes

$$\frac{N_1}{\sqrt{T_1^o}} = \frac{N_2}{\sqrt{T_2^o}}$$

Assuming $h_2^o/h_1^o = T_2^o/T_1^o$ and substituting equation (5) into it yield

$$\left(\frac{N_2}{N_1}\right)^2 = 1 + \frac{q}{h_1^o} \tag{7}$$

This equation is used to obtain M_2, the postcombustion Mach number. The critical value of M_2 is derived from $dN/dM = 0$, which from equation (6) becomes

$$M_c^2 = \left[\frac{\gamma}{\epsilon} - (\gamma - 1)\right]^{-1} \tag{8}$$

Stagnation Pressure Ratio of Burning

From equation (4),

$$\frac{P_2}{P_1} = \frac{A_1 G_1}{A_2 G_2}$$

which on the substitution of Crocco's relation

$$\frac{P_2}{P_1} = \left(\frac{A_2}{A_1}\right)^{\epsilon/(1-\epsilon)}$$

becomes

$$\frac{P_2}{P_1} = \left(\frac{G_1}{G_2}\right)^{\epsilon} \tag{9}$$

Also,

$$\frac{A_2}{A_1} = \left(\frac{G_1}{G_2}\right)^{1-\epsilon} \tag{10}$$

Then,

$$\frac{P_2}{P_1} = \left(\frac{G_1}{G_2}\right)^{\epsilon} \left(\frac{X_2}{X_1}\right)^{\gamma/(\gamma-1)}$$

where

$$X = 1 + \frac{\gamma - 1}{2} M^2$$

or

$$\left(\frac{P_2^o}{P_1^o}\right)^{(\gamma-1)/\gamma} = \frac{G_1^*}{G_2^*} \tag{11}$$

where

$$G^* = \frac{G\epsilon^{(\gamma-1)/\gamma}}{X}$$

Specific Impulse

Velocity of the jet at point 3 after expansion follows from sketch (p) and equation (5):

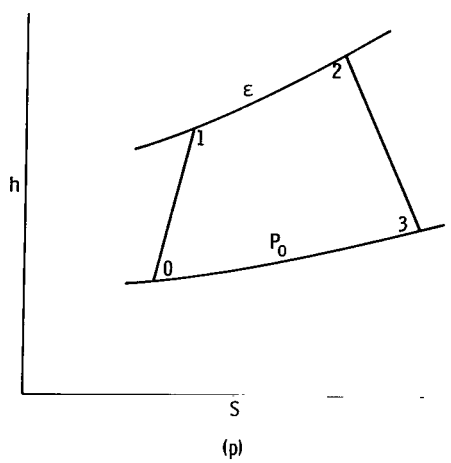

(p)

$$\frac{V_3^2}{2gJ} = h_3^o - h_3 = h_3^o\left(1 - \frac{1}{X_3}\right)$$

$$= h_2^o\left(1 - \frac{1}{X_3}\right) = \left(h_1^o + q\right)\left(1 - \frac{1}{X_3}\right)$$

Since

$$X_3^{\gamma/(\gamma-1)} = \frac{P_3^o}{P_3} = \frac{P_3^o}{P_0} = X_0^{\gamma/(\gamma-1)}\,\frac{P_1^o}{P_0^o}\,\frac{P_2^o}{P_1^o}\,\frac{P_3^o}{P_2^o}$$

it follows that

$$V_3^2 = 2gJ\left(h_1^o + q\right)\left[1 - \frac{1}{X_0}\left(\frac{P_0^o}{P_1^o}\,\frac{P_1^o}{P_2^o}\,\frac{P_2^o}{P_3^o}\right)^{(\gamma-1)/\gamma}\right] \tag{12}$$

and then

$$I_s = \frac{V_3 - V_0}{g \frac{\text{fuel}}{\text{air}}} \tag{13}$$

Critical Epsilon

Substituting equation (8) into (6) gives the value of N function at the critical point:

$$N_c^2 = \frac{1}{4\epsilon\gamma} \frac{1}{1 - \epsilon \frac{\gamma - 1}{2\gamma}} \tag{14}$$

Deriving an explicit expression for M from equation (6) yields

$$M^2 = \frac{1 - 2\epsilon\gamma N^2 \pm \sqrt{1 - 4N^2\epsilon\gamma\left(1 - \epsilon\gamma \frac{\gamma - 1}{2\gamma^2}\right)}}{2\gamma^2\left(N^2 - \frac{\gamma - 1}{2\gamma^2}\right)}$$

When the numerator and denominator are multiplied by

$$1 - 2\epsilon\gamma N^2 \mp \sqrt{1 - 4N^2\epsilon\gamma\left(1 - \epsilon\gamma \frac{\gamma - 1}{2\gamma^2}\right)}$$

it follows that

$$M^2 = \frac{4\epsilon^2\gamma^2 N^2\left(N^2 - \frac{\gamma - 1}{2\gamma^2}\right)}{2\gamma^2\left(N^2 - \frac{\gamma - 1}{2\gamma^2}\right)\left[1 - 2\epsilon\gamma N^2 \mp \sqrt{1 - 4N^2\epsilon\gamma\left(1 - \epsilon\gamma \frac{\gamma - 1}{2\gamma^2}\right)}\right]}$$

Using this equation and equation (14) gives

$$\frac{2\epsilon^2 N^2}{M^2} + 2\epsilon\gamma N^2 = 1 \pm \sqrt{1 - \frac{N^2}{N_c^2}}$$

or

$$2\epsilon\left(\frac{\epsilon}{M^2} + \gamma\right) = \left(1 \pm \sqrt{1 - \frac{N^2}{N_c^2}}\right)\frac{1}{N^2}$$

Multiplying both sides of the equation by N_c^2 yields

$$\frac{\gamma + \dfrac{\epsilon}{M^2}}{\gamma + \dfrac{\epsilon}{M_c^2}} = \frac{N_c^2}{N^2}\left(1 \pm \sqrt{1 - \frac{N^2}{N_c^2}}\right)$$

$$= \frac{M_c^2}{M^2}\frac{G}{G_c}$$

However,

$$\frac{N^2}{N_c^2} = \frac{M^2 X G_c^2}{M_c^2 X_c G^2}$$

which means that

$$\frac{X}{X_c} = \frac{N^2}{N_c^2}\frac{M_c}{M^2}\frac{G^2}{G_c^2} = \frac{N^2}{N_c^2}\frac{M_c^2}{M^2}\frac{M^4}{M_c^4}\frac{N_c^4}{N^4}\left(1 \pm \sqrt{1 - \frac{N^2}{N_c^2}}\right)^2 = \frac{N_c^2}{N^2}\frac{M^2}{M_c^2}\left(1 \pm \sqrt{1 - \frac{N^2}{N_c^2}}\right)^2$$

Hence, it follows that

$$\frac{\frac{1}{M^2} + \frac{\gamma - 1}{2}}{\frac{1}{M_c^2} + \frac{\gamma - 1}{2}} = \frac{N_c^2}{N^2}\left(1 \pm \sqrt{1 - \frac{N^2}{N_c^2}}\right)^2$$

or

$$\frac{\frac{F^2}{M^4}}{\left(\frac{F^2}{M^4}\right)_c} = \frac{(1 \pm \cos \alpha)^2}{\sin^2 \alpha}$$

where

$$\frac{N}{N_c} = \sin \alpha$$

Hence,

$$\frac{M^2}{F} = \left(\frac{M^2}{F}\right)_c \frac{\sin \alpha}{1 \pm \cos \alpha} \tag{15}$$

Substituting M_1 on the left hand side of equation (15) and

$$\sin \alpha = \frac{N_1}{N_c} = \frac{1}{\sqrt{1 + \frac{q}{h_1^o}}}$$

on the right hand side will give the value of M_c. Then from equation (8) the critical ϵ is obtained.

Hence this equation makes it possible to obtain directly the duct configuration that will secure a critical burning for a given M_1, heat condition, and stagnation enthalpy.

Mixing Equations

An algebraic treatment of the three conservation equations is now presented (see sketch (f), p. 15).

First, from the conservation of mass,

$$m_1 + m_j = m_m$$

In a manner similar to the way equation (2) was obtained, this can be put in the form

$$\frac{P_1 A_1 \gamma_1 F_1}{\sqrt{\gamma_1 R_1 T_1^o}} + \frac{P_j A_j \gamma_j F_j}{\sqrt{\gamma_j R_j T_j^o}} = \frac{P_m A_m \gamma_m F_m}{\sqrt{\gamma_m R_m T_m^o}} \tag{16}$$

Second, from the conservation of momentum,

$$\frac{1}{g}[m_m V_m - m_1 V_1 - m_j V_j] = P_1 A_1 + P_j A_j - P_m A_m + \int_1^m P\, dA \tag{17}$$

If it is assumed that the Crocco relation holds,

$$\frac{P}{P_1} = \left(\frac{A}{A_1 + A_j}\right)^{\epsilon/(1-\epsilon)}$$

then

$$\int_1^m P\, dA = \int_1^m P_1 \left(\frac{A}{A_1 + A_j}\right)^{\epsilon/(1-\epsilon)} dA = (1 - \epsilon)[P_m A_m - P_1(A_1 + A_j)] \tag{18}$$

Substituting equation (18) into equation (17) gives

$$\frac{1}{g}[m_m V_m - m_1 V_1 - m_j V_j] = P_1 A_1 + P_j A_j - P_1 A_0 - \epsilon P_m A_m + \epsilon P_1 (A_1 + A_j)$$

$$\epsilon P_m A_m + \frac{m_m V_m}{g} = \frac{m_1 V_1}{g} + \epsilon P_1 A_1 + \frac{m_j V_j}{g} + \epsilon P_1 A_j + P_j A_j - P_1 A_j$$

$$= \frac{m_1 V_1}{g} + \epsilon P_1 A_1 + \frac{m_j V_j}{g} + \epsilon P_1 A_j + P_j A_j - P_1 A_j + \epsilon P_j A_j - \epsilon P_j A_j$$

$$= \frac{m_1 V_1}{g} + \epsilon P_1 A_1 + \frac{m_j V_j}{g} + \epsilon P_j A_j + (P_j - P_1) A_j (1 - \epsilon)$$

$$= \frac{m_1 V_1}{g} + \epsilon P_1 A_1 + \frac{m_j V_j}{g} + P_j A_j \left[\epsilon + \left(1 - \frac{P_1}{P_j} \right) (1 - \epsilon) \right]$$

$$= \frac{m_1 V_1}{g} + \epsilon P_1 A_1 + \frac{m_j V_j}{g} + \epsilon_j P_j A_j$$

where

$$\epsilon_j = \epsilon + \left(1 - \frac{P_1}{P_j} \right) (1 - \epsilon)$$

Since $V = M\sqrt{g\gamma RT}$ and $m = PAM\gamma\sqrt{g}/\sqrt{\gamma RT}$, the previous equation can be put in the following form:

$$P_m A_m \left(\epsilon + \gamma_m M_m^2 \right) = P_1 A_1 \left(\epsilon + \gamma_1 M_1^2 \right) + P_j A_j \left(\epsilon_j + \gamma_j M_j^2 \right)$$

or

$$P_m A_m G_m = P_1 A_1 G_1 + P_j A_j G_j \tag{19}$$

where

$$G = \epsilon + \gamma M^2$$

From this form of the conservation of momentum equation,

$$\frac{P_m}{P_1} = \frac{A_1 G_1 + \frac{P_j}{P_1} A_j G_j}{A_m G_m}$$

but

$$A_m = (A_1 + A_j) A_m^*$$

where

$$A_m^* = \frac{A_m}{A_1 + A_j}$$

Hence,

$$\frac{P_m}{P_1} = \frac{A_1 G_1 + \frac{P_j}{P_1} A_j G_j}{(A_1 + A_j) A_m^* G_m} = \frac{G_{av}}{A_m^* G_m} \tag{20}$$

where

$$G_{av} = \frac{A_1 G_1 + \frac{P_j}{P_1} A_j G_j}{A_1 + A_j} = \frac{\overline{A}_1 G_1 + \frac{P_j}{P_1} G_j}{\overline{A}_1 + 1} \tag{21}$$

From Crocco's relation,

$$\frac{P_m}{P_1} = (A_m^*)^{\epsilon/(1-\epsilon)}$$

so

$$\frac{P_m}{P_1} = \left(\frac{G_{av}}{G_m} \frac{1}{P_m/P_1} \right)^{\epsilon/(1-\epsilon)}$$

Hence

$$\frac{P_m}{P_1} = \left(\frac{G_{av}}{G_m}\right)^{\epsilon} \tag{22}$$

and

$$A_m^* = \left(\frac{G_{av}}{G_m}\right)^{1-\epsilon} \tag{23}$$

Third, since

$$m = \frac{PA\gamma F\sqrt{g}}{\sqrt{\gamma RT^o}} = \frac{PA\gamma F\sqrt{g}}{\sqrt{\gamma J \frac{\gamma - 1}{\gamma} h^o}} \tag{24}$$

and equation (19) can be put in the form

$$P_1 A_1 \frac{F_1}{N_1} + P_j A_j \frac{F_j}{N_j} = P_m A_m \frac{F_m}{N_m}$$

one can substitute equation (24) into this equation with the result

$$m_1 \sqrt{\frac{\gamma_1 - 1}{\gamma_1^2}} \frac{\sqrt{h_1^o}}{N_1} + m_j \frac{\sqrt{h_j^o}}{N_j} \sqrt{\frac{\gamma_j - 1}{\gamma_j^2}} = m_m \frac{\sqrt{h_m^o}}{N_m} \sqrt{\frac{\gamma_m - 1}{\gamma_m^2}} \tag{25}$$

From conservation of energy,

$$m_1 h_1^o + m_j h_j^o = m_m h_m^o \tag{26}$$

and this equation can be put into the form

$$\frac{h_m^o}{h_j^o} = \frac{1 + \bar{m}_1 \dfrac{h_1^o}{h_j^o}}{1 + \bar{m}_1} = \frac{1 + \bar{m}_1 \Delta}{1 + \bar{m}_1} \tag{27}$$

Substituting equation (27) into equation (25) gives

$$\sqrt{\frac{\gamma_1 - 1}{\gamma_1^2}} \frac{m_1 \sqrt{h_1^o}}{N_1} + \sqrt{\frac{\gamma_j - 1}{\gamma_j^2}} \frac{m_j \sqrt{h_j^o}}{N_j} = \sqrt{\frac{\gamma_m - 1}{\gamma_m^2}} \frac{m_m \sqrt{h_j^o}}{N_m} \frac{\sqrt{1 + \bar{m}_1 \Delta}}{\sqrt{1 + \bar{m}_1}} \tag{28}$$

This is the fundamental equation for evaluation of mixing duct end Mach number M_m when the entrainment ratio $\bar{m}_1$, stagnation enthalpy ratio of two flows Δ, and Mach numbers of both flows are given. By simple transformation, equation (28) can be put in the form (with the assumption $\gamma_1 = \gamma_m = \gamma_j$)

$$\frac{\bar{m}_1}{1 + \bar{m}_1} \left(\frac{N_m}{N_1}\right)^2 = \left[1 - \frac{1}{1 + \sqrt{\bar{m}_1 \Delta} \left(\sqrt{\bar{m}_1} \dfrac{N_j}{N_1}\right)}\right]^2 \left(1 + \frac{1}{\bar{m}_1 \Delta}\right) \tag{29}$$

or

$$\frac{N_j}{N_m} = \frac{1}{\sqrt{(1 + \bar{m}_1)(1 + \bar{m}_1 \Delta)}} + \frac{\bar{m}_1 \sqrt{\Delta}}{\sqrt{(1 + \bar{m}_1)(1 + \bar{m}_1 \Delta)}} \frac{N_j}{N_1} \tag{30}$$

where

$$\bar{m}_1 = \bar{A}_1 \frac{P_1}{P_j} \frac{F_1}{F_j} \frac{1}{\sqrt{\Delta}}$$

Stagnation Pressure Ratio During Mixing

The stagnation pressure ratio of the mixing process is now evaluated. From conservation of momentum equation (19)

$$\frac{P_m A_m F_m}{N_m} = \frac{P_1 A_1 F_1}{N_1} + \frac{P_j A_j F_j}{N_j}$$

it follows that

$$\frac{P_m}{P_1} = \frac{N_m}{A_m F_m}\left(\frac{A_1 F_1}{N_1} + \frac{P_j}{P_1}\frac{A_j F_j}{N_j}\right)$$

$$= \frac{N_m}{A_m F_m}\left(\frac{A_1 F_1}{N_1} + \frac{P_j}{P_1}\frac{A_j}{A_1} A_1 \frac{F_j}{F_1}\frac{F_1}{N_j}\right)$$

Solving equation (24) for PAF and substituting in the previous equation yield

$$\frac{P_m}{P_1} = \frac{N_m A_1 F_1}{A_m F_m}\left(\frac{1}{N_1} + \frac{1}{\overline{m}_1\sqrt{\Delta}}\frac{1}{N_j}\right) \qquad \text{if } \gamma = \text{constant}$$

$$= \frac{A_1}{A_m}\frac{F_1}{F_m}\left(\frac{N_m}{N_1} + \frac{N_m}{N_j \overline{m}_1\sqrt{\Delta}}\right) \tag{31}$$

Now since

$$\frac{A_1}{A_m} = \frac{A_1}{A_1 + A_j}\frac{A_1 + A_j}{A_m} = \frac{\overline{A}_1}{1 + \overline{A}_1}\frac{1}{A_m^*} \tag{32}$$

substituting equation (32) into equation (31) in turn results in

$$A_m^* \frac{P_m}{P_1} = \frac{\overline{A}_1}{1 + \overline{A}_1}\frac{F_1}{F_m}\left(\frac{N_m}{N_1} + \frac{N_m}{N_j \overline{m}_1\sqrt{\Delta}}\right) \tag{33}$$

Crocco's relation gives

$$\frac{P_m}{P_1} = (A_m^*)^{\epsilon/(1-\epsilon)}$$

From this

$$A_m^* = \left(\frac{P_m}{P_1}\right)^{(1-\epsilon)/\epsilon}$$

and

$$\frac{P_m}{P_1} A_m^* = \left(\frac{P_m}{P_1}\right)^{1/\epsilon} \tag{34}$$

Substituting equation (34) into equation (33) results in

$$\frac{P_m}{P_1} = \left(\frac{\overline{A_1}}{1+\overline{A_1}}\right)^{\epsilon} \left(\frac{F_1}{F_m}\right)^{\epsilon} \left(\frac{N_m}{N_1} + \frac{N_m}{N_j \overline{m}_1 \sqrt{\Delta}}\right)^{\epsilon}$$

Then the stagnation pressure ratio will be given by

$$\frac{P_m^o}{P_1^o} = \left(\frac{\overline{A_1}}{1+\overline{A_1}}\right)^{\epsilon} \left(\frac{N_m}{N_1} + \frac{N_m}{N_j \overline{m}_1 \sqrt{\Delta}}\right)^{\epsilon} \frac{F_1^{\epsilon}}{X_1^{\gamma/(\gamma-1)}} \frac{X_m^{\gamma/(\gamma-1)}}{F_m^{\epsilon}}$$

$$= \left(\frac{\overline{A_1}}{1+\overline{A_1}}\right)^{\epsilon} \left(1 + \frac{N_1}{N_j \overline{m}_1 \sqrt{\Delta}}\right)^{\epsilon} \frac{N_m^{\epsilon}}{F_m^{\epsilon}} \frac{F_1^{\epsilon}}{N_1^{\epsilon}} \frac{X_m^{\gamma/(\gamma-1)}}{X_1^{\gamma/(\gamma-1)}}$$

Hence, since $N/F = 1/G$,

$$\left(\frac{P_m^o}{P_1^o}\right)^{(\gamma-1)/\gamma} = \left(\frac{\overline{A_1}}{1+\overline{A_1}}\right)^{\epsilon(\gamma-1)/\gamma} \left(1 + \frac{N_1}{N_j \overline{m}_1 \sqrt{\Delta}}\right)^{\epsilon(\gamma-1)/\gamma} \frac{G_1^*}{G_m^*} \tag{35}$$

where, as in equation (11),

$$G^* = \frac{G^{\epsilon(\gamma-1)/\gamma}}{X}$$

Burning After Mixing

Conservation of energy is

$$m_m h_m^o + m_1 q = m_m h_2^o$$

where

$$m_m = m_1 + m_j$$

Hence,

$$(\overline{m}_1 + 1)h_m^o + \overline{m}_1 q = (\overline{m}_1 + 1)h_2^o \tag{36}$$

During mixing, the conservation equation was

$$h_j^o + \overline{m}_1 h_1^o = (\overline{m}_1 + 1)h_m^o \tag{37}$$

Substituting equation (37) into equation (36) gives

$$h_j^o + \overline{m}_1 h_1 + \overline{m}_1 q = (\overline{m}_1 + 1)h_2^o \tag{38}$$

Then

$$\left(\frac{N_2}{N_m}\right)^2 = \frac{T_2^o}{T_m^o} = \frac{h_j^o + \bar{m}_1 h_1^o + \bar{m}_1 q}{h_j^o + \bar{m}_1 h_1^o} = \frac{1 + \bar{m}_1 \Delta + \bar{m}_1 \frac{q}{h_j^o}}{1 + \bar{m}_1 \Delta} = \frac{1 + \bar{m}_1 \Delta^\infty}{1 + \bar{m}_1 \Delta} \tag{39}$$

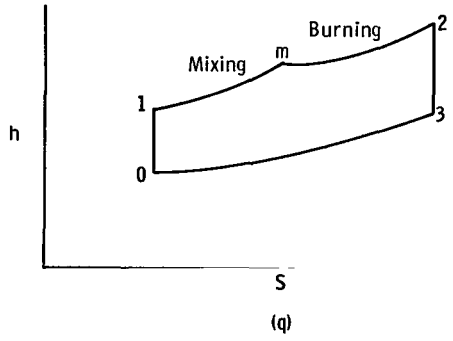

(q)

where

$$\Delta^\infty = \Delta + \frac{q}{h_j^o}$$

The velocity that can be developed at point 3 (see sketch (q)) will be given by

$$\frac{V_3^2}{2gJ} = h_3^o - h_3 = h_3^o \left(1 - \frac{1}{X_3}\right) = h_2^o \left(1 - \frac{1}{X_3}\right) = \frac{h_j^o + \bar{m}_1 h_1^o + \bar{m}_1 q}{1 + \bar{m}_1} \left(1 - \frac{1}{X_3}\right)$$

Then gross jet thrust per unit primary mass flow is

$$(\bar{m}_1 + 1)V_3 = \sqrt{2gJ}\ (1 + \bar{m}_1) \sqrt{\frac{h_j^o + \bar{m}_1 h_1^o + \bar{m}_1 q}{1 + \bar{m}_1}} \sqrt{1 - \left(\frac{P_0}{P_3^o}\right)^{(\gamma-1)/\gamma}}$$

$$= \sqrt{2gJ}\ (1 + \bar{m}_1) \sqrt{h_1^o + q + \frac{h_j^o - h_1^o - q}{1 + \bar{m}_1}} \sqrt{1 - \left(\frac{P_0}{P_3^o}\right)^{(\gamma-1)/\gamma}} \tag{40}$$

and

$$I_s = \frac{(\bar{m}_1 + 1)V_3 - \bar{m}_1 V_0}{g\left(1 + \bar{m}_1 \frac{\text{fuel}}{\text{air}}\right)} \tag{41}$$

Burning While Mixing Process

The primary jet here is stoichiometric and the fuel has to be supplied for the stoichimetric combustion of the entrained secondary flow. The mass of fuel is considered negligible as compared to $m_1 + m_j$.

The conservation of energy equation can be stated as

$$m_1 h_1^o + m_j h_j^o + m_1 q = m_2 h_2^o$$

or

$$\bar{m}_1 h_1^o + h_j^o + \bar{m}_1 q = (\bar{m}_1 + 1) h_2^o$$

This is the same as equation (38); hence, the same equation for the jet thrust as shown in (40) is obtained. The specific impulse is

$$I_s = \frac{(\bar{m}_1 + 1)V_3 - \bar{m}_1 V_0}{g}$$

The primary jet here is fuel-rich and constitutes the only source of fuel for the secondary flow.

REFERENCES

1. Pool, H. L.; and Charyk, J. V.: Progress of Experimental Study of Ejector Action and Mixing Involving Reacting Fluids. Tech. Rep. No. 25, Princeton University, Project Squid, Sept. 1950.

2. Kennedy, E. D.: Mixing of Compressible Fluids. J. Appl. Mech., vol. 28, no. 3, Sept. 1961, pp. 335-338.

3. Kiselev, B. M.: Calculation of One-Dimensional Gas Flows. Tech. Rep. No. F-TS-1209-IA, Wright-Patterson AFB, Intelligence Dept., Jan. 1949. (Trans. of Prikl. Matematika i Mekhanika, vol. 11, 1947, pp. 177-192.)

4. Glassman, Irvin; and Charyk, Joseph: The Ramrocket. Jet Propulsion Engines, vol. 12 of High Speed Aerodynamics and Jet Propulsion, O. E. Lancaster, ed., Princeton University Press, 1959, pp. 625-661.

"The aeronautical and space activities of the United States shall be conducted so as to contribute . . . to the expansion of human knowledge of phenomena in the atmosphere and space. The Administration shall provide for the widest practicable and appropriate dissemination of information concerning its activities and the results thereof."

—NATIONAL AERONAUTICS AND SPACE ACT OF 1958

NASA SCIENTIFIC AND TECHNICAL PUBLICATIONS

TECHNICAL REPORTS: Scientific and technical information considered important, complete, and a lasting contribution to existing knowledge.

TECHNICAL NOTES: Information less broad in scope but nevertheless of importance as a contribution to existing knowledge.

TECHNICAL MEMORANDUMS: Information receiving limited distribution because of preliminary data, security classification, or other reasons.

CONTRACTOR REPORTS: Technical information generated in connection with a NASA contract or grant and released under NASA auspices.

TECHNICAL TRANSLATIONS: Information published in a foreign language considered to merit NASA distribution in English.

TECHNICAL REPRINTS: Information derived from NASA activities and initially published in the form of journal articles.

SPECIAL PUBLICATIONS: Information derived from or of value to NASA activities but not necessarily reporting the results of individual NASA-programmed scientific efforts. Publications include conference proceedings, monographs, data compilations, handbooks, sourcebooks, and special bibliographies.

Details on the availability of these publications may be obtained from:

SCIENTIFIC AND TECHNICAL INFORMATION DIVISION

NATIONAL AERONAUTICS AND SPACE ADMINISTRATION

Washington, D.C. 20546